buildings

MDPI

Article

Shear Strength of Headed Stud Connectors in Self-Compacting Concrete with Recycled Coarse Aggregate

Samoel Mahdi Saleh [1,*] and Fareed Hameed Majeed [2]

[1] Department of Civil Engineering, University of Basrah, Basrah 61004, Iraq
[2] College of Engineering, University of Basrah, Basrah 61004, Iraq; fareed.majeed@uobasrah.edu.iq
* Correspondence: samoel.saleh@uobasrah.edu.iq

Abstract: This study investigated the use of self-compacting concrete (SCC) made with recycled coarse aggregates (RCAs), which represents a trend of producing environment-friendly concrete, integrated with hot-rolled steel sections by means of headed stud shear connectors in composite structures. Therefore, thirty-six push-out test specimens were examined to assess the shear strength and behavior of the headed stud connectors embedded in RCA-SCC, with the concrete compressive strength, stud diameter, and RCA ratio as the main variables. Four ratios of RCAs ranging from 0 to 60% were used to produce concrete with three different compressive strengths (25, 33, and 40 MPa) for each one. It was found that the use of SCC with RCAs had a negative effect on the shear strength of headed stud connectors. This negative effect could be reduced by increasing the concrete compressive strength and/or the stud diameter. Similarly, a reduction in the shear stiffness of the tested specimens was inversely proportional to the RCA ratio, while the ultimate slip was directly proportional to the RCA ratio. An evaluation of the test results was made by comparing them with those determined by Eurocode 4 and AASHTO LRFD.

Keywords: push-out test; headed stud; recycle coarse aggregate; self-compacting concrete

Citation: Saleh, S.M.; Majeed, F.H. Shear Strength of Headed Stud Connectors in Self-Compacting Concrete with Recycled Coarse Aggregate. *Buildings* **2022**, *12*, 505. https://doi.org/10.3390/buildings12050505

Academic Editors: Binsheng (Ben) Zhang and Wei (David) Dong

Received: 11 March 2022
Accepted: 17 April 2022
Published: 19 April 2022

1. Introduction

Construction innovation combined with advancements in material properties and technologies has enabled humans to pursue the challenges of building higher and more complicated structures. The steel–concrete composite beam represents one of the fastest, least expansive, and most eco-friendly structural members that are commonly used in different types of high buildings as well as bridge decks. The structural behavior of such beams relies primarily on the efficiency of the shear connections used, which is achieved by different types of mechanical connectors through which longitudinal shear between the steel beam and the reinforced concrete slab is transferred. Among the different sorts of shear connectors, headed stud connectors are the most commonly utilized in composite beams.

Many studies have been carried out to investigate the strength of stud shear connectors through the use of push-out tests. Ollgaard et al. [1] investigated the behavior and strength of stud connectors embedded in normal-weight concrete and lightweight concrete. It was found that the concrete strength and modulus of elasticity have the most significant effect on the shear strength of the stud connectors. Lam and El-Lobody [2] proposed a finite element model for the push-out test to perform a parametric study on the effects of variations in concrete strength and the diameter of stud connectors on the load–slip behavior of the shear connection in steel–concrete composite beams. Shim et al. [3] performed push-out tests along with finite element modeling to examine the shear capacity and load–slip behavior of stud connectors embedded in fiber-reinforced concrete and high-strength concrete. Compared with the values presented in current codes of practice, the experimental results showed that the thickness of the stud welding and the concrete reinforcement might affect the shear capacity of stud connections. After reviewing a large number of pull-out and

push-out test results, Pallares and Hajjar [4] proposed formulas for the limit states of headed stud connectors under shear, tension, and shear and tension combined. Qi et al. [5] experimentally and numerically investigated the effect of initial damage in a stud connector on its shear capacity. It was observed that even though the stud area was significantly reduced when the damage section was located at 0.5 d, where d is the shank diameter from the root, the shear capacity was not affected by the degree of damage. Yang et al. [6] presented push-out tests to examine the shear performance and load–slip behavior of large-diameter and high-strength stud connectors. They concluded that welded stud connectors with high strengths and large diameters could undergo ductile failure when the welding process and concrete strength employed were the same as those used in conventional welded stud connectors. The static behavior of headed stud connectors in ultra-high-performance concrete (UHPC) was investigated experimentally and numerically by Qi et al. [7]. They observed that the shear capacity of the headed studs resulted from the concrete wedge block shear contribution and the stud shear contribution. The shear stiffness of the headed studs in UHPC was increased by about 60% more than that in normal-strength concrete. Moreover, they showed that the shear strength of the studs in UHPC was not affected by the reduction in stud height from six times to twice its diameter. He et al. [8] investigated the shear stiffness of the headed stud shear connectors that were embedded in different types of concrete with different compressive strengths. They proposed a formula to predict the shear stiffness of headed studs based on the results of 206 push-out tests available in the literature. It was observed that the elastic moduli of concrete and steel and the stud diameter played major roles in the shear stiffness of headed stud connectors. In general, it seems that the type and mechanical properties of concrete are the main factors affecting the strength of the stud shear connection. Therefore, studying the strength and behavior of such shear connection with the use of increasingly popular types of concrete containing waste materials and industrial byproducts is important to develop more efficient and economical steel–concrete composite beams.

Since its initial production in the 1980s, self-compacting concrete (SCC) has been used extensively, especially for high-rise buildings in which concrete compaction may be problematic or not possible. Unlike conventional concrete (CC), SCC is at a higher level of workability, and the issues of bleeding and segregation are evident in this type of concrete, providing a significant improvement in the productivity and quality of construction work. On the other hand, because of the environmental benefits, the impact of potential economic interest in technology for processing concrete with recycled materials is rapidly increasing. Since the volume of produced concrete is dominated by coarse aggregates, one of the most common ways to produce environment-friendly concrete is by using crushed concrete generated by the demolition of aging infrastructures and buildings, such as coarse aggregates. Hence, different experimental and numerical studies have been performed to examine the behavior and mechanical properties of self-compacting concrete with recycled coarse aggregate (RCA-SCC) in recent years. Matias et al. [9] investigated the variations in the mechanical properties of concrete with recycled coarse aggregates (RCAs), comparing them with those in conventional concrete with natural coarse aggregates (NCAs) in the presence of superplasticizers. They showed some strengths and weaknesses of concrete with RCAs related to the changes in the replacement ratio for replacing natural aggregates with recycled ones. An investigation by Tang et al. [10] assessed the strength, workability, and fracture properties of SCC with various ratios of RCA to total coarse aggregates. With the exception of a slight reduction in Young's modulus, they observed that the evaluated properties of SSC had little or no negative impact at RCA utilization levels ranging from 25% to 50%. In 2019, the workability and strength of SSC containing partial/full RCAs using ultrafine recycled powder and silica fume as ternary blended cement were investigated by Singh et al. [11]. They showed that the results of compressive and flexural strengths for various mixtures of RCA-SCC were promising. However, the results of the study showed that up to 10% of ultrafine recycled powder can be used according to its effect on concrete workability. Tang et al. [12] studied the fresh and hardened properties of RCA-SCC in

structural applications, considering the effect of using a lithium silicate solution as a surface treatment for RCAs. In comparison with untreated RCA-SCC, they concluded that treated RCA-SCC had improved mechanical properties. In 2020, Garcia et al. [13] discussed the workability and mechanical properties of SCC with different substation ratios of RCAs and compared the results with control concrete. The study showed that RCAs could be used in the production of SSC with minimal losses in its characteristics. In 2020, Dawood [14] studied fresh and hardened SCC made with RCAs using two types of fine materials (limestone powder and silica fume). Slump flow and J-ring tests, in addition to fresh density, were used to assess the fresh properties of the concrete, while the hardened properties were evaluated according to the compressive strength, splitting tensile strength, and flexural strength tests as well as dry density and water absorption. It was shown that the use of RCAs in SCC adversely affected the workability and hardening properties of the concrete depending on the replacement ratio of RCAs used. Kathirvel et al. [15] investigated the effect of replacing (partially) the natural aggregates with RCAs and silica fume with cement on the mechanical properties of the SCC. The used RCAs were treated with magnesium sulfate solution to reduce the effect of the absorptive nature and high porousness of the RCA surfaces. The results revealed that the splitting tensile strength and compressive strength of SCC with 60% RCA content were reduced by about 35% and 34%, respectively.

A review of previous studies on headed stud shear connectors clearly indicated that the use of headed stud shear connectors with RCA-SCC in composite structures has yet to be reported. None of the research works published previously have presented the use of RCA-SCC with steel sections and headed stud connectors integrated as composite beam systems. Hence, the present work was undertaken to assess the shear strength and behavior of headed stud connectors embedded in self-compacting concrete made with recycled coarse aggregates so that design recommendations could be made. The assessment was based on the fabrication and testing of thirty-six push-out test specimens, taking into account the effect of several factors, such as the replacement ratio of RCAs, the concrete compressive strength, and the diameter of the headed stud. The test results were compared with those predicted by Eurocode 4 and AASHTO LRFD bridge design specifications.

2. Experimental Work

2.1. Test Specimens

Thirty-six push-out test specimens were fabricated to assess the shear strength and load–slip behavior of stud shear connectors embedded in SCC slabs made with RCAs. As shown in Figure 1, all the test specimens were assembled from a 500 mm length of an HE200B European standard steel section attached to an RCA-SCC slab with a thickness of 150 mm, a width of 500 mm, and a height of 500 mm on each side by one row of two 100 mm long headed stud connectors. Each concrete slab was reinforced by embedding four longitudinal and four horizontal 10 mm steel reinforcement bars on each face. The main variables taken into consideration in this study were the RCA replacement ratio, concrete compressive strength, and stud diameter. The stud tensile strength and rebar and steel section yield stresses were considered one-level factors. This permitted the direct evaluation of the RCA ratio and concrete properties on the shear connection strength. The adopted specimens' designation, as shown in Table 1, was represented using the letter S followed by a six-digit number. The first two digits represent the replacement ratio of RCAs used in the specimen's concrete. The second and third two digits refer to the target concrete compressive strength and the stud diameter, respectively.

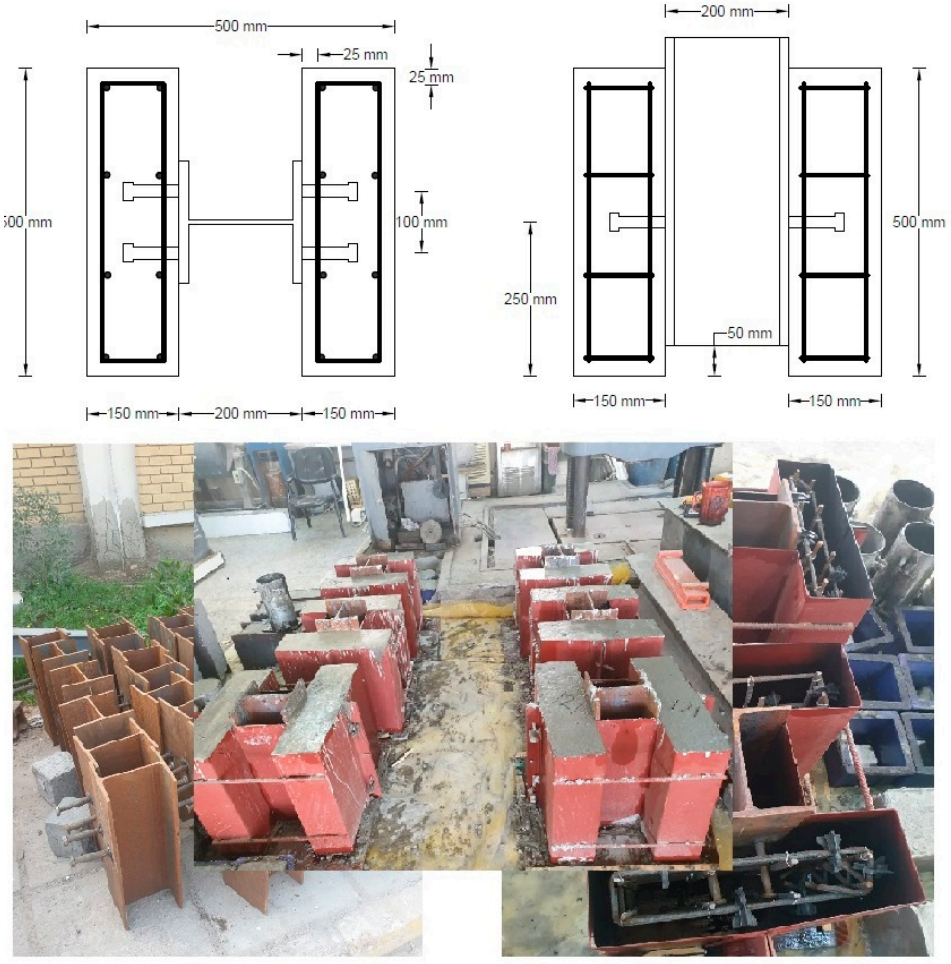

Figure 1. Details of push-out test specimens.

Table 1. Details of push-out test specimens.

Specimen's Designation	RCA%	Compressive Strength (MPa)	Concrete Properties Tensile Strength (MPa)	Modulus of Elasticity (GPa)	Stud Diameter (mm)
S002512					12
S002516		26.0	3.1	24.6	16
S002520					20
S003312					12
S003316	0	33.6	3.5	29.4	16
S003320					20
S004012					12
S004016		41.7	4.2	31.4	16
S004020					20
S202512					12
S202516		25.9	3.1	23.5	16
S202520					20
S203312					12
S203316	20	33.7	3.4	27.8	16
S203320					20
S204012					12
S204016		41.2	4.1	30.6	16
S204020					20

Table 1. *Cont.*

Specimen's Designation	RCA%	Compressive Strength (MPa)	Concrete Properties Tensile Strength (MPa)	Modulus of Elasticity (GPa)	Stud Diameter (mm)
S402512					12
S402516		25.7	3.0	20.1	16
S402520					20
S403312					12
S403316	40	33.1	3.4	26.2	16
S403320					20
S404012					12
S404016		41.0	4.0	28.5	16
S404020					20
S602512					12
S602516		25.9	3.1	19.3	16
S602520					20
S603312					12
S603316	60	34.1	3.6	25.7	16
S603320					20
S604012					12
S604016		40.8	4.0	27.9	16
S604020					20

2.2. Material Properties

To accomplish the goals of the present work, twelve mixes of self-compacting concrete and recycled coarse aggregates (RCA-SCC) were needed; this was achieved by replacing 0, 20%, 40%, and 60% of the required natural coarse aggregates with RCAs, considering three ultimate compressive strengths (25 MPa, 33 MPa, and 40 MPa) for each replacement ratio. The designed concrete mixes consisted of cement, natural fine aggregate (sand), natural coarse aggregate (NCA), recycled coarse aggregate (RCA), limestone powder (LP), superplasticizer (SP), and water, and individual mixes had different ratios of these materials. The details of the RCA-SCC mixes adopted after numerous trials for the present study are shown in Table 2.

Table 2. Details of concrete mix materials.

f'_c (MPa)	W/C Ratio	Water (kg/m^3)	Cement (kg/m^3)	Sand (kg/m^3)	NCA (kg/m^3)	RCA (kg/m^3)	CG (%)	LP (kg/m^3)	SP (L/m^3)
25	0.39	120	310	1200	700	0	0	150	6.4
	0.40	125	310	1200	560	132	20	150	6.2
	0.42	130	310	1200	420	264	40	150	6.1
	0.39	120	310	1200	280	396	60	150	6.2
33	0.35	125	360	1120	700	0	0	150	7.5
	0.36	130	360	1120	560	132	20	150	7.2
	0.38	135	360	1120	420	264	40	150	7.0
	0.35	126	360	1120	280	396	60	150	7.2
40	0.34	145	430	1010	700	0	0	150	10.0
	0.35	150	430	1010	560	132	20	150	10.5
	0.36	155	430	1010	420	264	40	150	10.5
	0.34	148	430	1010	280	396	60	150	10.0

The loose bulk density, aggregate crushed value, and other physical properties of the fine and coarse aggregates are listed in Table 3. The recycled coarse aggregates were obtained from the demolition of several reinforced concrete blocks with compressive strengths ranging between 25 MPa and 35 MPa, which were used for previous experimental tests in the institute laboratory, whereas natural river gravel was adopted as the NCA in the present work. The size gradings of the NCAs, RCAs, and sand were chosen according to the ASTM C33-03 specification considering a maximum size of 12.5 mm for both NCAs and RCAs and 2.36 mm for sand, as shown in Figure 2.

Table 3. Properties of fine and coarse aggregates.

Material	Max. Size (mm)	Specific Gravity	Sulfate Content (%)	Absorption (%)	Loose Bulk Density (kg/m^3)	Aggregate Crushed Value * (%)
Sand	2.36	2.64	0.110	0.98	1610	—-
NCA	12.5	2.60	0.061	1.11	1560	19.5
RCA	12.5	2.45	0.071	6.51	1320	30.4

* These values were evaluated according to BS 812-110: 1990.

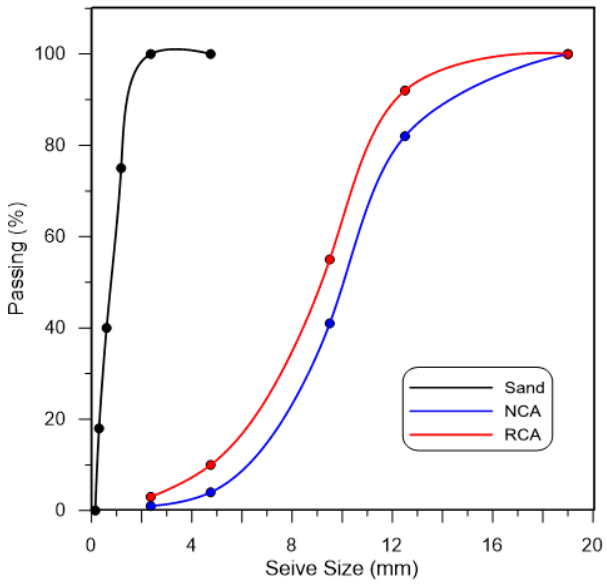

Figure 2. Particle size analysis curves of fine and coarse aggregates.

When the push-out test specimens were fabricated, the fresh properties of SCC mixes were examined by the slump flow test, L-box test, and sieve segregation test, which were adopted according to the EN 206-9: 2010 and EN 12350 specifications, as shown in Table 4. Moreover, twelve 150 mm dia. × 300 mm standard cylinders were cast with each concrete batch according to ASTM C 873-02 in order to evaluate the mechanical properties of the concrete slabs in which the stud connectors were embedded. These cylinders, along with the push-out test specimens, were moistly cured for seven days and then air-cured until the testing date at the age of 28 days. The concrete compressive strength (f'_c), the splitting tensile strength (f_t), and the elastic modulus of elasticity for each concrete batch were evaluated according to the standard tests recommended by ASTM C 873-02, ASTM C469-02a, and ASTM C496-04, respectively; see Table 1. The ultimate tensile strength of the used studs was specified according to the results of a standard tension test provided by the supplier and was 448 MPa for the 20 mm studs and about 440 MPa for both the 16 mm and 12 mm studs.

Table 4. Fresh properties of SCC.

f'_c (MPa)	RCA Ratio (%)	Slump Flow Value (mm)	Blocking Ratio	Sieve Segregation (%)
25	0	750	0.92	10.2
	20	730	0.93	9.1
	40	700	0.94	8.5
	60	700	0.92	7.2
33	0	740	0.94	9.8
	20	740	0.91	8.6
	40	730	0.93	6.8
	60	730	0.92	6.1
40	0	740	0.94	9.5
	20	720	0.92	8.2
	40	730	0.94	6.1
	60	730	0.91	5.8

2.3. Push-Out Tests

A 100-ton capacity universal testing machine (TORSEE) was adopted to test the push-out specimens by applying monotonic loading with a loading rate of about 5.0 kN/min. The applied load was measured by a 75-ton load cell (MT711), whereas the vertical relative slips between the steel beam and the concrete slabs were measured at each load increment by two linear variable differential transducers (LVDTs) fixed on both sides of the steel beam, as shown in Figure 3.

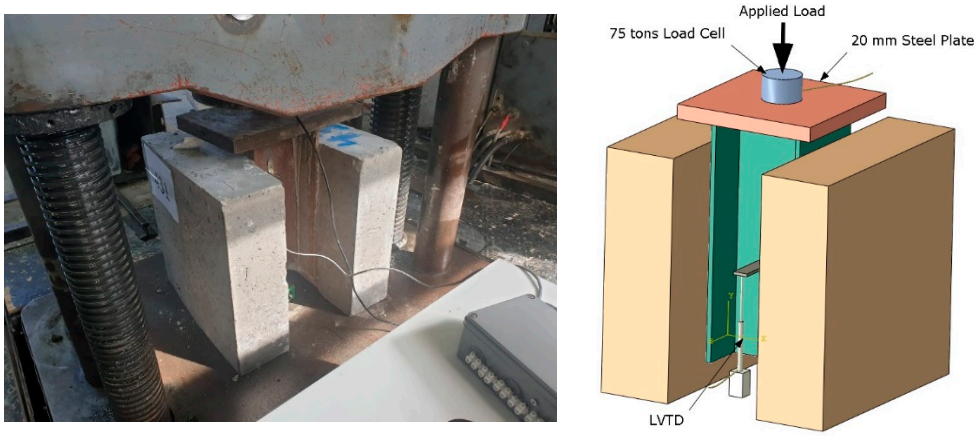

Figure 3. Description of push-out test setup.

3. Test Results and Discussion

3.1. Modes of Failure and Shear Strength

All specimens were subjected to additional loading after the ultimate load was reached until one or both slabs separated from the steel beam. As shown in Figure 4, two failure modes were observed in the present work. The first mode of failure, by which all the specimens failed except three, started with concrete compression failure around the studs, followed by the studs yielding. This failure occurred at a relatively large slip. On the other hand, stud shear failure was observed in specimens S203320, S403316, and S404020, representing another mode of failure. The studs of these specimens were sheared off at the root and remained embedded in the concrete slabs with small values of slip compared with the results of other specimens. These two modes of failure were demonstrated in previous studies conducted by Lam and EI-Loboby [2] and Xue et al. [16].

(**a**) (**b**)

Figure 4. Failure modes of tested specimens. (**a**) Combined failure of concrete and stud. (**b**) Studs' shear failure at root.

The stud ultimate shear load, the corresponding ultimate slip, and the mode of failure for the tested specimens are shown in Table 5. In light of the test results, it can be noted that the shear strength of headed studs significantly increased by about 33% and 49% with an increase in the concrete compressive strength from 26 MPa to 41 MPa in the push-out test specimens for SCC with an RCA ratio of zero and 12 mm and 16 mm stud diameters, respectively. Moreover, the change in the stud diameter from 12 mm to 20 mm in the specimens with a compressive concrete strength of about 26 MPa and an RCA ratio of zero developed an increasing ratio in the stud shear strength of about 71%. The same findings were obtained from the results of other specimens with an RCA ratio of zero in their concrete slabs. However, it can be seen that the increase in the RCA ratio in the specimen's concrete slab developed a reduction in the ultimate shear strength of the headed studs regardless of the stud diameter or concrete compressive strength. When the RCA ratio changed from 0 to 60%, the stud shear capacity was reduced by a ratio of about 39% for specimens with a concrete compressive strength of 26 MPa and a 12 mm stud diameter. This ratio was reduced to 33% and 27% when the concrete strength increased to 34 MPa and 41 MPa, respectively. The change in the RCA ratio from 0 to 60% in specimens S002512 and S602512 reduced the stud shear strength from 62.7 kN to 38.2 kN with a reduction ratio of about 40%, but a change in the stud diameter from 12 mm to 20 mm, as seen in specimens S002520 and S602520, controlled the negative effect of increasing the RCA ratio so that the reduction ratio was about 26%. It can be observed from the test results that the ultimate shear strength of the test specimens increased considerably when the concrete compressive strength and/or stud diameter increased, even with an increase in the RCA ratio of the concrete slab specimens; see Figure 5.

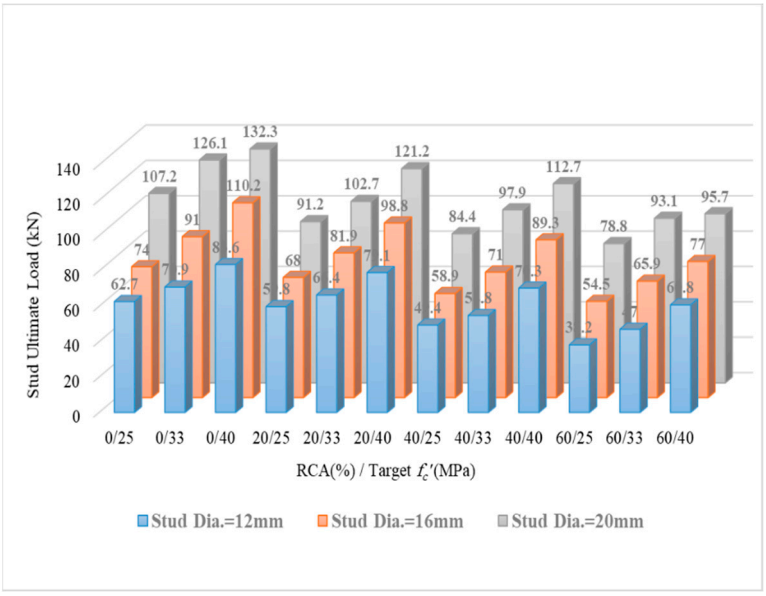

Figure 5. Variations in the stud ultimate shear loads with the RCA ratio.

Table 5. Experimental results of the test specimens.

Specimen's Designation	Stud Ultimate Shear Load, P_u (kN)	Ultimate Slip, S_u (mm)	Mode of Failure
S002512	62.7	5.65	Combined failure
S002516	74.0	4.99	Combined failure
S002520	107.2	4.48	Combined failure
S003312	70.9	5.16	Combined failure
S003316	91.0	4.50	Combined failure
S003320	126.1	4.31	Combined failure
S004012	83.6	4.83	Combined failure
S004016	110.2	3.78	Combined failure
S004020	132.3	4.20	Combined failure

Table 5. *Cont.*

Specimen's Designation	Stud Ultimate Shear Load, P_u (kN)	Ultimate Slip, S_u (mm)	Mode of Failure
S202512	59.8	5.90	Combined failure
S202516	68.0	5.16	Combined failure
S202520	91.2	4.61	Combined failure
S203312	66.4	5.61	Combined failure
S203316	81.9	4.62	Combined failure
S203320	102.7	1.99	Stud failure (root)
S204012	79.1	5.12	Combined failure
S204016	98.8	3.91	Combined failure
S204020	121.2	4.65	Combined failure
S402512	49.4	5.96	Combined failure
S402516	58.9	5.53	Combined failure
S402520	84.4	4.92	Combined failure
S403312	54.8	6.01	Combined failure
S403316	71.0	2.97	Stud failure (root)
S403320	97.9	4.66	Combined failure
S404012	70.3	5.64	Combined failure
S404016	89.3	4.26	Combined failure
S404020	112.7	2.17	Stud failure (root)
S602512	38.2	6.20	Combined failure
S602516	54.5	5.71	Combined failure
S602520	78.8	5.01	Combined failure
S603312	47.0	6.15	Combined failure
S603316	65.9	4.72	Combined failure
S603320	93.1	4.82	Combined failure
S604012	60.8	5.90	Combined failure
S604016	77.0	4.81	Combined failure
S604020	95.7	4.91	Combined failure

3.2. Load–Slip Relationships

Figures 6–8 show the effects of the RCA ratio on the load–slip behaviors for the tested specimens with different combinations of concrete compressive strength and stud diameter. Three different stages were observed in the load–slip curves, which started with a linear stage of up to 65–75% of the ultimate load followed by a nonlinear stage with increasing the slip while the load approached the ultimate load. After the ultimate load was achieved, the specimens were subjected to further deformation accompanied by a decrease in the load, which represents the third stage of the load–slip curve. The shear stiffness of the tested specimens, which represents the slope of the linear portion of the load–slip curve, was significantly inversely affected by the RCA ratio of their concrete slabs. This effect was clearly shown by the increase in the concrete compressive strength and/or the stud diameters of the tested specimens.

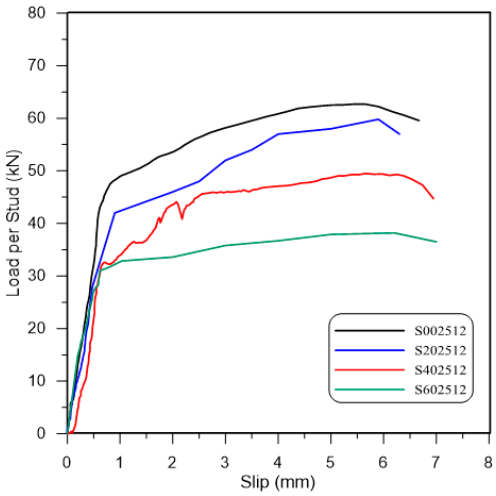

Figure 6. Load–slip curves for the specimens with f'_c = 25 MPa and 12 mm stud diameter.

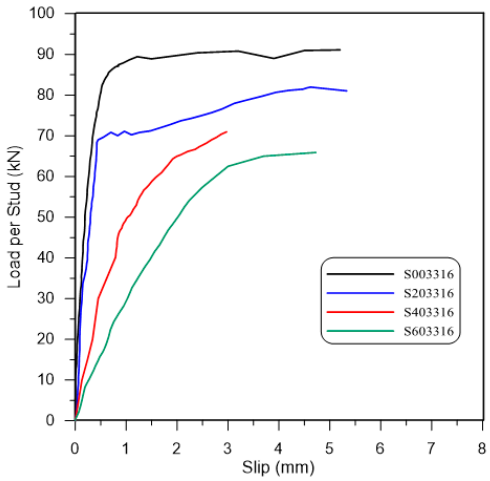

Figure 7. Load–slip curves for the specimens with f'_c = 33 MPa and 16 mm stud diameter.

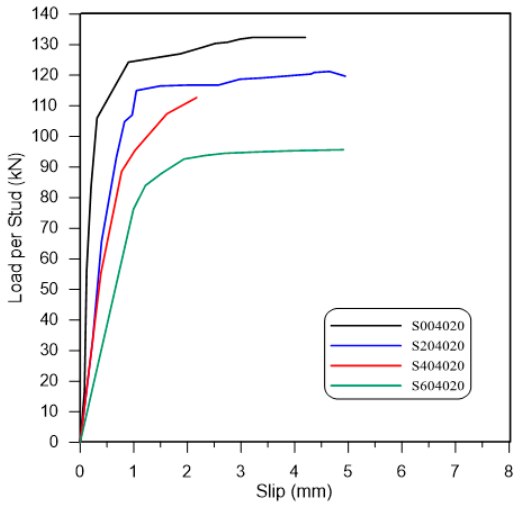

Figure 8. Load–slip curves for the specimens with f'_c = 40 MPa and 20 mm stud diameter.

The recorded ultimate slip for the tested specimens, except those sustaining stud shear failure, was directly proportional to the increase in the RCA ratio and inversely proportional to the concrete compressive strength and/or stud diameter, as shown in Figure 9. It can be seen that the specimens with a 12 mm stud diameter exhibited slip values relatively greater than those with a 20 mm stud diameter, which was demonstrated by several previous studies, e.g., Badie et al. [17], Lee et al. [18], and Shim et al. [19]. This may be related to the mode of failure observed in such specimens, which started with a concrete failure followed by stud yielding. Accordingly, the headed studs with a diameter of 12 mm were subjected to a smaller concrete bearing resistance and a larger deformation than those with a diameter of 20 mm. Therefore, the ultimate slip values for the tested specimens with the same stud diameter were reduced with increasing concrete compressive strength. The same reason may be attributed to the increase in the ultimate slip and the decrease in the shear stiffness in the tested specimens with increasing RCA amounts because of the reduction in the concrete bearing resistance in the region that supported the headed studs, which was a result of the higher aggregate crashing value of RCAs in comparison with NCAs. However, the variations in the ultimate slip with an increased RCA ratio may reduce with increased concrete compressive strength.

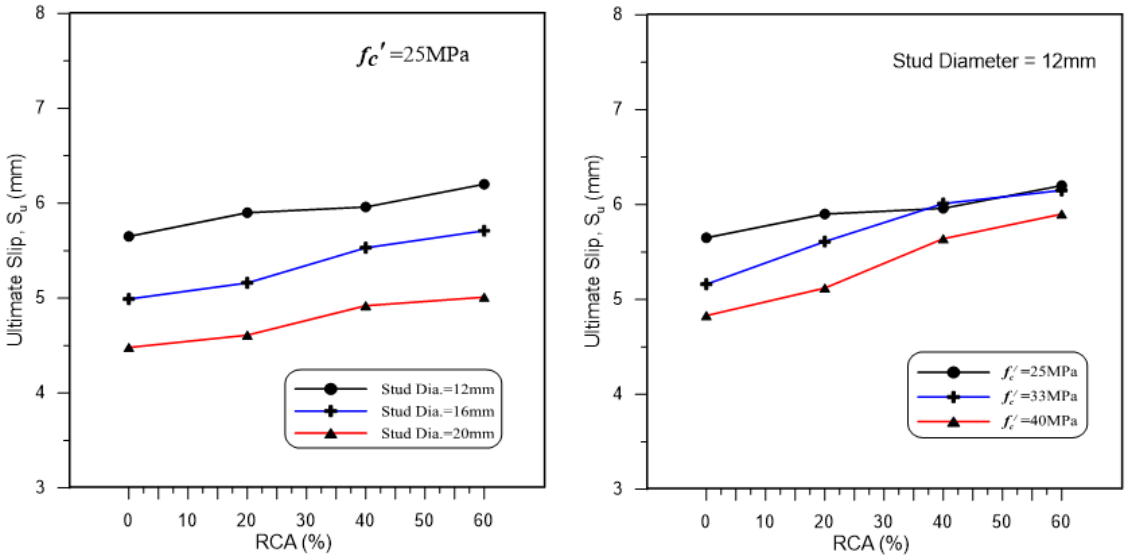

Figure 9. Variations in the ultimate slip with RCA ratio.

4. Evaluation of the Test Results

EN 1994-1-1 (Eurocode 4) [20] specifies the ultimate shear strength of headed stud connectors according to the following equation, where d and f_u are the stud diameter and ultimate tensile strength of stud material, and E_c and f_c' are the concrete modulus of elasticity and compressive strength, respectively.

$$P_u = \min\left(0.29\alpha d^2\sqrt{E_c f_c'},\ 0.2\pi d^2 f_u\right) \quad (1)$$

The factor α is a function of the headed stud diameter and length, which is equal to 1.0 when the length of the headed stud is larger than four times its diameter.

On the other hand, the ultimate shear strength of the headed stud that is recommended in AASHTO LRFD [21] can be determined according to the following Equation:

$$P_u = 0.125\pi d^2\sqrt{E_c f_c'} \le \frac{\pi d^2}{4} f_u \quad (2)$$

Table 6 lists the comparative results of the predicted stud shear capacity using the Eurocode 4 and AASHTO LRFD approaches with the push-out test results. It can be seen that the Eurocode 4 approach gave more conservative shear capacities than those predicted by AASHTO LRFD. Most of the evaluated shear capacities by using Equation (1) were underestimated by up to 50% compared with the test results, whereas the values that were calculated using Equation (2) varied from the overestimated values by 41% and from the underestimated values by up to 40% compared with the experimental results. The difference between the estimated shear strength of a headed stud based on the design codes and those found in the experimental work may be explained by the fact that the design codes evaluate the shear strength on the basis of the minimum shear resistance of one of the two materials, the headed stud or the concrete slab, while the observed shear strengths of the tested specimens were based on the contributions of both the headed stud and the concrete slab. Moreover, the two equations above were adopted for the shear strength of headed studs in normal concrete.

Table 6. Experimental results of the test specimens.

Specimen's Designation	Ultimate Shear Capacity (kN)			P_{EN}/P_u	P_{AA}/P_u
	Test, P_u	Eurocode 4, P_{EN}	AASHTO, P_{AA}		
S002512	62.7	33.3	45.1	0.53	0.72
S002516	74.0	59.3	80.2	0.8	1.08
S002520	107.2	92.6	125.4	0.86	1.17
S003312	70.9	39.8	49.8	0.56	0.7
S003316	91.0	70.8	88.5	0.78	0.97
S003320	126.1	110.6	138.2	0.88	1.1
S004012	83.6	39.8	49.8	0.48	0.6
S004016	110.2	70.8	88.5	0.64	0.8
S004020	132.3	110.6	138.2	0.84	1.04
S202512	59.8	32.6	44.1	0.55	0.74
S202516	68.0	57.9	78.4	0.85	1.15
S202520	91.2	90.5	122.5	0.99	1.34
S203312	66.4	39.8	49.8	0.6	0.75
S203316	81.9	70.8	88.5	0.86	1.08
S203320	102.7	110.6	138.2	1.08	1.35
S204012	79.1	39.8	49.8	0.5	0.63
S204016	98.8	70.8	88.5	0.72	0.9
S204020	121.2	110.6	138.2	0.91	1.14
S402512	49.4	30.0	40.6	0.61	0.82
S402516	58.9	53.4	72.3	0.91	1.23
S402520	84.4	83.4	112.9	0.99	1.34
S403312	54.8	38.9	49.8	0.71	0.91
S403316	71.0	69.1	88.5	0.97	1.25
S403320	97.9	108.0	138.2	1.1	1.41
S404012	70.3	39.8	49.8	0.57	0.71
S404016	89.3	70.8	88.5	0.79	0.99
S404020	112.7	110.6	138.2	0.98	1.23
S602512	38.2	29.5	40	0.77	1.05
S602516	54.5	52.5	71.1	0.96	1.3
S602520	78.8	82.0	111.1	1.04	1.41
S603312	47.0	39.1	49.8	0.83	1.06
S603316	65.9	69.5	88.5	1.05	1.34
S603320	93.1	108.6	138.2	1.17	1.48
S604012	60.8	39.8	49.8	0.65	0.82
S604016	77.0	70.8	88.5	0.92	1.15
S604020	95.7	110.6	138.2	1.16	1.44
Mean				0.82	1.06
Standard Deviation				0.19	0.25

5. Conclusions

The present study was conducted to assess the shear strength and behavior of headed stud connectors embedded in the self-compacting concrete made with recycled coarse aggregates, which represents a trend of producing environment-friendly concrete. The assessment was based on the fabrication and testing of thirty-six push-out test specimens, taking into account the effect of the replacement ratio of RCA, the concrete compressive strength, and the diameter of the headed stud. The stud's ultimate shear strength, ultimate slip, and load–slip behavior were evaluated and compared with those predicted by the Eurocode 4 and AASHTO LRFD equations. The following conclusions were drawn:

1. The ultimate shear strength of headed stud shear connectors embedded in SCC is directly proportional to the concrete compressive strength and/or the diameter of headed stud connectors, regardless of the RCA ratio used.
2. The use of SCC with RCAs has a negative effect on the shear strength of headed stud connectors. This negative effect may be reduced by increasing the concrete compressive strength and/or the stud diameter.
3. The shear stiffness and ultimate slip of the tested push-out specimens were inversely proportional to the RCA ratio because of the reduction in the concrete bearing resistance in the region that supported the headed studs, which occurred as a result of the higher aggregate crashing value of RCAs in comparison with NCAs.
4. The increase in the ultimate slip due to the RCA ratio may be controlled by increasing the concrete compressive strength.

Author Contributions: Conceptualization and methodology, S.M.S. and F.H.M.; resources and experimental work, F.H.M., analysis of experimental results and writing, S.M.S. All authors have read and agreed to the published version of the manuscript.

Funding: This research received no external funding.

Conflicts of Interest: The authors declare no conflict of interest.

References

1. Ollgaard, J.G.; Slutter, R.G.; Fisher, J.W. Shear strength of stud connectors in lightweight and normal-weight concrete. *AISC Eng.* **1971**, *8*, 55–64.
2. Lam, D.; El-Lobody, E. Behavior of headed stud shear connectors in composite beam. *J. Struct. Eng.* **2005**, *131*, 96–107. [CrossRef]
3. Shim, H.B.; Chung, K.S.; Jang, S.H.; Lee, J.H.; Park, S.T. Pushout tests on shear studs in high strength concrete. In Proceedings of the Fracture Mechanics of Concrete and Concrete Structures, Seoul, Korea, 23–28 May 2010.
4. Palleres, L.; Hajjar, J. Headed steel studs anchors in composite structures, Part 1: Shear. *J. Constr. Steel Res.* **2010**, *66*, 198–212. [CrossRef]
5. Qi, J.; Wang, J.; Li, M.; Chan, L. Shear capacity of stud shear connectors with initial damage: Experiment, FEM model and theoretical formulation. *Steel Compos. Struct.* **2017**, *25*, 79–92.
6. Yang, F.; Liu, Y.; Li, Y. Push-out tests on large diameter and high strength welded stud connectors. *Adv. Civil Eng.* **2018**, *2018*, 1–12. [CrossRef]
7. Qi, J.; Hu, Y.; Wand, J.; Li, W. Behavior and strength of headed stud shear connectors in ultra-high performance concrete of composite bridges. *Front. Struct. Civil Eng.* **2019**, *13*, 1138–1149. [CrossRef]
8. He, J.; Lin, Z.; Liu, Y.; Xu, X.; Xin, H.; Wang, S. Shear stiffness of headed studs on structural behaviors of steel-concrete composite girders. *Steel Compos. Struct.* **2020**, *36*, 553–568.
9. Matias, D.; Brito, J.; Rosa, A.; Pedro, D. Mechanical properties of concrete produced with recycled coarse aggregate—Influence of the use of superplasticizers. *Constr. Build. Mater.* **2013**, *44*, 101–109. [CrossRef]
10. Tang, W.C.; Ryan, P.C.; Cui, H.Z.; Liao, W. Properties of self-compacting concrete with recycled coarse aggregate. *Adv. Mater. Sci. Eng.* **2016**, *2016*, 2761294. [CrossRef]
11. Singh, A.; Arora, S.; Sharma, V.; Bhardwaj, B. Workability retention and strength development of self-compacting recycled aggregate concrete using ultrafine recycled powders and silica fume. *J. Hazard. Toxic Radioact. Waste* **2019**, *23*, 1–12. [CrossRef]
12. Tang, W.; Khavarian, M.; Yousefi, A.; Chan, R.W.K.; Cui, H. Influence of surface treatment of recycled aggregate on material properties and bond strength of self-compacting concrete. *Sustainability* **2019**, *11*, 4182. [CrossRef]
13. Garcia, R.M.; Romero, M.I.G.; Pozo, J.M.M. Recycled aggregate for self-compacting concrete production: A feasible option. *Materials* **2020**, *13*, 868. [CrossRef] [PubMed]
14. Dawood, E.T. Behavior of self-compacting concrete produced form recycled aggregate. *AIP Conf. Proc.* **2020**, *2213*, 020023. [CrossRef]
15. Kathirvel, P.; Murali, G.; Vatin, N.I.; Abid, S.R. Experimental study on self- compacting fibrous concrete comprising magnesium sulphate solution treated recycled aggregates. *Materials* **2022**, *15*, 340. [CrossRef]
16. Xue, W.C.; Ding, M.; Wang, H.; Luo, Z.W. Static behavior and theoretical model of stud shear connectors. *J. Bridge Eng.* **2008**, *13*, 623–634. [CrossRef]
17. Badie, S.S.; Tadros, M.K.; Kakish, H.F.; Splittgerber, D.L.; Baishya, M.C. Large shear studs for composite action in steel bridge girders. *J. Bridge Eng.* **2002**, *7*, 195–203. [CrossRef]
18. Lee, P.G.; Shim, C.S.; Chang, S.P. Static and fatigue behavior of large stud shear connectors for steel-concrete composite bridges. *J. Constr. Steel Res.* **2005**, *61*, 1270–1285. [CrossRef]
19. Shim, C.S.; Lee, P.G.; Yoon, T.Y. Static behavior of large stud shear connectors. *Eng. Struct.* **2004**, *26*, 1853–1860. [CrossRef]
20. *EN 1994-1-1*; Eurocode 4: Design of Composite Steel and Concrete Structures, Part 1-1: General Rules and Rules for Buildings. European Committee for Standardization (CEN): Brussels, Belgium, 2004.
21. AASHTO. *AASHTO LFRD Bridge Design Specifications*, 4th ed.; American Associate of State Highway and Transportation Officials: Washington, DC, USA, 2007.